THE ASTROPHYSICAL JOURNAL, 545:129–140, 2000 December 10

WHAT FRACTION OF GRAVITATIONAL LENS GALAXIES LIE IN GROUPS?

CHARLES R. KEETON, DANIEL CHRISTLEIN, AND ANN I. ZABLUDOFF
Steward Observatory, University of Arizona, 933 North Cherry Avenue, Tucson, AZ 85716
Received 2000 May 9; accepted 2000 July 17

ABSTRACT

We predict how the observed variations in galaxy populations with environment affect the number and properties of gravitational lenses in different environments. Two trends dominate: lensing strongly favors early-type galaxies, which tend to lie in dense environments, but dense environments tend to have a larger ratio of dwarf to giant galaxies than the field. The two effects nearly cancel, and the distribution of environments for lens and nonlens galaxies are not substantially different (lens galaxies are slightly less likely than nonlens galaxies to lie in groups and clusters). We predict that $\sim 20\%$ of lens galaxies are in bound groups (defined as systems with a line-of-sight velocity dispersion σ in the range $200 < \sigma < 500$ km s^{-1}), and another $\sim 3\%$ are in rich clusters ($\sigma > 500$ km s^{-1}). Therefore, at least $\sim 25\%$ of lenses are likely to have environments that significantly perturb the lensing potential. If such perturbations do not significantly increase the image separation, we predict that lenses in groups have a mean image separation that is $\sim 0\farcs2$ *smaller* than that for lenses in the field, and we estimate that 20–40 lenses in groups are required to test this prediction with significance. The tail of the distribution of image separations is already illuminating. Although lensing by galactic potential wells should rarely produce lenses with image separations $\theta \gtrsim 6''$, two such lenses are seen among 49 known lenses, suggesting that environmental perturbations of the lensing potential can be significant. Further comparison of theory and data will offer a direct probe of the dark halos of galaxies and groups and reveal the extent to which they affect lensing estimates of cosmological parameters.

Subject headings: galaxies: clusters: general — galaxies: halos — gravitational lensing

1. INTRODUCTION

Gravitational lensing of background sources by foreground galaxies offers a powerful probe of galaxy structure and evolution at intermediate redshifts ($0.3 \lesssim z \lesssim 1$; e.g., Keeton, Kochanek, & Falco 1998; Kochanek et al. 2000a). Lenses are also used to constrain the cosmological parameters H_0, Ω_M, and Ω_Λ (e.g., Falco, Kochanek, & Muñoz 1998; Helbig et al. 1999; Koopmans & Fassnacht 1999; Witt, Mao, & Keeton 2000, and references therein). These applications rely on accurate models of the mass distribution responsible for the lensing, but the models may be complicated by contributions of the lens galaxy's environment to the lensing potential, especially when the lens galaxy lies in a poor group or rich cluster of galaxies.

A crucial step in understanding how environment may affect lensing constraints on dark matter halos and cosmological parameters is determining the fraction of lens galaxies in groups and in clusters. The environments of most lenses are not known. Three lens galaxies are confirmed group members (PG 1115+080, B1422+231, and MG 0751+2716; Kundić et al. 1997a, 1997b; Tonry 1998; Tonry & Kochanek 1999), and another four lie in clusters (RX J0911+0551, RX J0921+4528, Q0957+561, and HST 1411+5221; Young et al. 1981; Fischer, Schade, & Barrientos 1998; Kneib, Cohen, & Hjorth 2000; Muñoz et al. 2000). While environmental effects have been included in models of some of these lenses (e.g., Schechter et al. 1997; Keeton & Kochanek 1997; Barkana et al. 1999; Bernstein & Fischer 1999; Chae 1999; Keeton et al. 2000a; Lehár et al. 2000), lens environments have not been addressed statistically (see Keeton, Kochanek, & Seljak 1997 for an initial analysis). In particular, previous predictions of the statistics of galaxy lenses could not examine environmental effects because they assumed an environment-independent galaxy luminosity function (e.g., Turner 1980; Turner, Ostriker, & Gott 1984; Fukugita & Turner 1991; Kochanek 1993a, 1996a, 1996b; Maoz & Rix 1993; Wallington & Narayan 1993; Falco et al. 1998; Quast & Helbig 1999; Helbig et al. 1999).

The existence of lenses in groups and clusters is not surprising. Lensing selects galaxies by mass and thus preferentially selects early-type galaxies, which are most common in dense environments (e.g., the morphology-density relation; Dressler 1980). However, recent studies suggest that richer environments tend to have a higher ratio of dwarf to giant galaxies than the field (Bromley et al. 1998b; Christlein 2000; Zabludoff & Mulchaey 2000), and dwarf galaxies are much poorer lenses than giant galaxies. The morphology-density relation increases the chance of having a lens in a group or cluster, while the dwarf-to-giant ratio decreases it, so the distribution of lens galaxy environments depends on how these two effects combine quantitatively.

In this paper, we examine how changes in the type and luminosity distribution of galaxies with environment ("population variations") affect lens statistics. Using new results that quantify the type and environment dependence of the galaxy luminosity function (Bromley et al. 1998a, 1998b; Christlein 2000), we obtain the first predictions of the distribution of lens galaxy environments and of statistical differences in the properties of lenses in different environments. We neglect contributions to the lensing potential from other galaxies and the extended dark halo of the group or cluster ("potential perturbations"), which introduce a tidal shear that distorts image configurations and a gravitational focusing that increases image separations (e.g., Schneider, Ehlers, & Falco 1992). This assumption not only simplifies the analysis, but also constitutes the null hypothesis as to whether potential perturbations contribute (statistically) to lensing.

The organization of the paper is as follows. In § 2 we

discuss the components of the statistical calculations, including galaxy luminosity functions and the gravitational lens model. In § 3 we use simple analytic results to highlight the trends of environmental effects in lens statistics. In § 4 we use empirical galaxy luminosity functions to obtain quantitative predictions of the environmental effects. Finally, in § 5 we offer a summary and discussion.

2. DATA AND METHODS

2.1. *Galaxy Populations*

We must formally describe a population of galaxies that can act as gravitational lens galaxies in order to compute the set of lenses they can produce. Depending on details of the observational sample, galaxies can be binned by type, environment, and/or redshift. Within each discrete bin, the distribution of galaxy luminosities is described using a smooth galaxy luminosity function (GLF) $\phi(L)$, such that $\phi(L)dL$ is the comoving number density of galaxies with luminosity between L and $L + dL$. The GLF is usually parameterized as a Schechter (1976) function with the form

$$\phi_i(L) = \frac{n_i^*}{L_i^*}\left(\frac{L}{L_i^*}\right)^{\alpha_i} e^{-L/L_i^*}, \quad (1)$$

where i labels the type, environment, and/or redshift bin. The GLF is described by a characteristic comoving number density n_i^*, a characteristic luminosity L_i^*, and a faint-end slope α_i. The differences between GLFs in different bins are characterized by differences in the Schechter parameters n_i^*, L_i^*, and α_i.

Current surveys are not large enough to bin galaxies by type, environment, and redshift simultaneously; only recently has it become possible to examine even two of the three quantities. Because we are interested in the effects of environment, we adopt the sample of galaxies from the Las Campanas Redshift Survey (LCRS; Shectman et al. 1996). This survey provides a large-volume, R-band–selected sample of the nearby universe that offers four benefits for our study. First, it samples down to an estimated completeness limit of $M_R = -17.5 + 5 \log h$, or nearly 3 mag below M^*. Second, its large volume offers a fair sample of environments from the field to groups and clusters. Third, its large number of galaxies means that galaxies can be binned by both type and environment with sufficient statistics to discriminate between GLFs in different bins.

The fourth benefit is that there are two independent and complementary analyses of type and environmental dependences in the LCRS GLFs. Bromley et al. (1998a, 1998b, hereafter collectively B98) classify galaxies using six type and two environment classes. They define six spectral types (which they call "clans") derived from a principal component analysis of important spectral features. The clans smoothly span the range from quiescent galaxies that have substantial absorption lines, 4000 Å breaks, and old stellar populations (clans 1 and 2) to star-forming galaxies with prominent emission lines and a significant fraction of young stars (clans 5 and 6). B98 define two environment categories based on the local three-dimensional number density of galaxies: "high-density" environments correspond roughly to groups and clusters of galaxies (identified using a friends-of-friends algorithm), while "low-density" environments include only galaxies that lie outside groups. Table 1 gives the parameters for the GLFs derived by B98.

TABLE 1

B98 Luminosity Function Parameters

Clan	Environment	α	$M^* - 5 \log h$	n^* ($10^{-3}\ h^3$ Mpc^{-3})
1.....	low-density	1.10	−20.06	0.18
	high-density	0.20	−20.48	0.21
2.....	low-density	0.17	−20.10	5.36
	high-density	−0.39	−20.39	2.61
3.....	low-density	−0.09	−19.81	7.79
	high-density	−0.58	−20.00	2.97
4.....	low-density	−0.65	−19.88	7.01
	high-density	−0.61	−19.78	3.10
5.....	low-density	−1.05	−19.80	3.70
	high-density	−1.61	−20.39	0.49
6.....	low-density	−1.94	−20.09	1.38
	high-density	−1.93	−20.14	0.56

Note.—Luminosity function parameters derived by B98 for their six spectral type "clans" and two environments.

The study by Christlein (2000, hereafter C00) uses a different scheme for classifying type and environment, placing more emphasis on environment than type. C00 defines two galaxy types, using the equivalent width of [O II] λ3727 Å to separate "emission-line" (EL; $\geq$5 Å) from "non–emission line" (NEL; $<$5 Å) galaxies. He defines environments by identifying groups (using a friends-of-friends algorithm) and classifying galaxies by the velocity dispersion of the group in which they reside. Table 2 gives the parameters for the GLFs derived by C00.

B98 and C00 find similar trends in the type and environment dependence of the GLF. The characteristic density n^* varies with both type and environment, but there is no obvious trend. The faint-end slope α systematically steepens from early- to late-type galaxies and from the field to denser environments, leading to an increase in the dwarf-to-giant ratio with local galaxy density. The fact that both studies

TABLE 2

C00 Luminosity Function Parameters

Galaxy Type	Group σ (km s^{-1})	α	$M^* - 5 \log h$	n^* ($10^{-4}\ h^3$ Mpc^{-3})
NEL.....	other	−0.079	−20.23	49.31
	50	0.202	−20.04	2.58
	150	0.070	−20.16	4.92
	250	−0.345	−20.40	5.68
	350	−0.334	−20.34	6.54
	450	−0.596	−20.59	2.63
	750	−0.909	−20.84	2.54
EL	other	−0.908	−20.14	63.74
	50	−0.870	−20.18	3.23
	150	−0.958	−20.30	4.84
	250	−0.932	−20.18	6.09
	350	−1.304	−20.49	3.39
	450	−0.708	−20.03	3.02
	750	−1.025	−20.17	2.58

Note.—Luminosity function parameters derived by C00 for two galaxy types and seven environment bins. One environment bin ("other") contains all galaxies that do not lie in groups. The remaining bins classify galaxies by the velocity dispersion σ of the group in which they reside. The five environment bins labeled 50, 150, 250, 350, and 450 km s^{-1} are 100 km s^{-1} wide and are labeled by the central value. The bin labeled 750 km s^{-1} includes the range $500 < \sigma < 1000$ km s^{-1}. Typical uncertainties are $\sim$0.2 in α and $\sim$0.2 mag in M^*; see C00 for details.

reveal similar trends using different galaxy classification techniques suggests that the trends are robust. Zabludoff & Mulchaey (2000) detect a similar variation in the dwarf-to-giant ratio with environment using a completely different sample of galaxies.

One drawback of the LCRS for our analysis is that the sample is drawn from the nearby universe ($\langle z \rangle \simeq 0.1$; Shectman et al. 1996), while most lens galaxies are found at redshifts between 0.3 and 1. There are, however, several independent studies of redshift evolution in the GLF (e.g., Lilly et al. 1995; Lin et al. 1999). We cannot use these studies directly because they are too small to permit environment classification, but we can apply the inferred redshift trends. We adopt as our main hypothesis that the only evolution is passive luminosity evolution, but we also examine how number density evolution would affect our conclusions.

2.2. *Lens Model*

The gravitational lens model specifies what kind of lensed images can be produced by a galaxy of a given luminosity, type, and environment. We adopt the standard singular isothermal sphere (SIS) lens model because of its analytic simplicity, and because it is consistent with stellar dynamical models (e.g., Rix et al. 1997b), X-ray galaxies (e.g., Fabbiano 1989), models of individual lens systems (e.g., Kochanek 1995; Grogin & Narayan 1996), and lens statistics (e.g., Maoz & Rix 1993; Kochanek 1993a, 1996a). The image separation θ produced by an SIS lens is independent of the impact parameter of the source relative to the lens and is given by (e.g., Schneider et al. 1992)

$$\theta = 8\pi\left(\frac{\sigma}{c}\right)^2 \frac{D_{ls}}{D_{os}}, \tag{2}$$

where σ is the velocity dispersion of the lens galaxy, and D_{os} and D_{ls} are proper motion distances from the observer to the source and from the lens to the source, respectively. (The distance ratio is the same if the two distances are taken to be angular diameter distances.) The cross section for multiple imaging (in angular units) is

$$\mathscr{A} = \frac{\pi}{4}\,\theta^2 . \tag{3}$$

It is convenient to introduce a characteristic angular scale for lensing,

$$\theta^* = 8\pi\left(\frac{\sigma^*}{c}\right)^2 , \tag{4}$$

which is the image separation produced by an L^* lens galaxy (with velocity dispersion σ^*) for a source at infinity.

The SIS lens model omits three features that are known to affect lensing: ellipticity in the lens galaxy, tidal shear from objects near the lens galaxy, and gravitational focusing (or "convergence") from the environment. Statistically, ellipticity and shear mainly affect the relative numbers of two- and four-image lenses (e.g., Keeton et al. 1997), which we do not differentiate. Convergence from the environment can increase image separations by a few percent up to $\sim 20\%$ (e.g., Bernstein & Fischer 1999). Our use of the SIS lens model amounts to an assumption that environmental contributions to the lensing potential do not affect lens statistics; thus, our results will serve as the null hypothesis when examining whether potential perturbations affect lens statistics.

To apply SIS lens models to galaxies classified by luminosity, we must convert from luminosity to velocity dispersion using empirical scaling relations such as the Faber-Jackson relation for early-type galaxies and the Tully-Fisher relation for late-type galaxies. Both relations have the form

$$\frac{L}{L^*} = \left(\frac{\sigma}{\sigma^*}\right)^{\gamma} . \tag{5}$$

For early-type galaxies, combining the Faber-Jackson relation with the gravitational lens statistics yields (Kochanek 1993a)

$$\gamma \approx 4, \quad \sigma^* = 220 \pm 20 \text{ km s}^{-1} , \quad \theta^* = 2\farcs79 , \tag{6}$$

which also agrees with dark matter models for the stellar dynamics of elliptical galaxies (Kochanek 1994). For spiral galaxies, we find that combining the R-band GLF (Tables 1 and 2) with the R-band Tully-Fisher relation of Sakai et al. (2000) yields

$$\gamma = 3.6 \pm 0.3 , \quad \sigma^* = 100 \pm 6 \text{ km s}^{-1} , \quad \theta^* = 0\farcs58 . \tag{7}$$

This is an updated version of the normalization given by Fukugita & Turner (1991). The normalization differences between early- and late-type galaxies are basically differences in mass. Early-type galaxies tend to have more mass for a given luminosity (a higher mass-to-light ratio) than late-type galaxies, at least within the optical radius, so they tend to have higher velocity dispersions and produce larger image separations.

We assume that σ^* and γ do not change with redshift. Under passive luminosity evolution, the mass scale given by σ^* does not evolve. In addition, high-redshift studies of the Tully-Fisher relation (e.g., Vogt et al. 1996; Rix et al. 1997a) and of the fundamental plane of elliptical galaxies (e.g., van Dokkum & Franx 1996; Kelson et al. 1997; van Dokkum et al. 1998; Kochanek et al. 2000a) suggest that γ does not evolve. Even if the no-evolution assumption is not entirely justified, Mao (1991), Mao & Kochanek (1994), and Rix et al. (1994) have shown that lens statistics are affected by evolution only if there are dramatic changes in the population of early-type galaxies at redshifts $z < 1$.

2.3. *Statistics*

We want to compute statistical properties of both nonlens and lens galaxies. For simplicity, in this discussion we refer to the set of galaxies in a particular type and environment bin i as galaxy population i. The total number density, n_i, and luminosity density, $\rho_{L,i}$, for galaxy population i are obtained by integrating over the luminosity function,

$$n_i = \int_{L_{\rm cut}}^{\infty} \phi_i(L)dL = n_i^*\,\Gamma(1+\alpha_i;\, L_{\rm cut}/L_i^*) , \tag{8}$$

$$\rho_{L,i} = \int_{L_{\rm cut}}^{\infty} L\phi_i(L)dL = n_i^*\,L_i^*\,\Gamma(2+\alpha_i;\, L_{\rm cut}/L_i^*) , \tag{9}$$

where the integrals include only galaxies brighter than some completeness limit $L_{\rm cut}$, and they can be evaluated in terms of incomplete Γ functions.

For lens galaxies, the main statistical quantity is the optical depth for a source at redshift z_s to be lensed by

galaxy population i (e.g., Turner et al. 1984; Fukugita & Turner 1991),

$$\tau_i(z_s) = \frac{1}{4\pi} \int dV \int dL \, \mathscr{A}_i(L, z_l, z_s) \phi_i(L) \, , \tag{10}$$

where ϕ_i is the GLF for the galaxy population and $\mathscr{A}_i(L, z_l, z_s)$ is the cross section for multiple imaging by a lens of luminosity L at redshift z_l. In order to compute the number of lenses expected in any real survey, the optical depth would have to be modified by a "magnification bias" factor to account for lenses in which the source is intrinsically fainter than the flux limit but magnified above the threshold (e.g., Turner 1980; Turner et al. 1984). For the SIS lens model, magnification bias simply yields a coefficient multiplying the optical depth, and the coefficient is the same for all galaxy populations. Because we are mainly interested in the relative number of lenses produced by different galaxy populations, we can neglect magnification bias.

If there is no redshift evolution in the GLF other than passive luminosity evolution, the optical depth and other related quantities can be computed analytically. The following results were originally given by Gott, Park, & Lee (1989), Fukugita & Turner (1991), Kaiser & Tribble (1991), and Kochanek (1993b); we have modified them to introduce an explicit luminosity cut at the completeness limit, $L_{\rm cut}$. The total optical depth is

$$\tau_i(z_s) = \tau_i^* \, f(z_s) \Gamma(1 + \alpha_i + 4\gamma_i^{-1}; L_{\rm cut}/L_i^*) \, , \tag{11}$$

where

$$\tau_i^* = 16\pi^3 r_{\rm H}^3 n_i^* \left(\frac{\sigma_i^*}{c} \right)^4 , \tag{12}$$

$$f(z_s) = \frac{1}{r_{\rm H}^3} \int_0^{D_{os}} \frac{(D_{ol} D_{ls}/D_{os})^2}{(1 + \Omega_k D_{ol}^2/r_{\rm H}^2)^{1/2}} \, dD_{ol} \, , \tag{13}$$

where D_{ol} is the proper-motion distance from the observer to the lens, $r_{\rm H} = c/H_0$ is the Hubble distance, and $\Omega_k = 1 - \Omega_M - \Omega_\Lambda$ is the curvature density. Writing the optical depth as in equation (11) emphasizes how the various dependences separate. The characteristic optical depth τ_i^* contains the characteristic number density n_i^* and mass scale σ_i^* for the galaxy population. The Γ function contains the shape information from the GLF (the faint-end slope α_i) and the L-σ scaling relation (the Faber-Jackson or Tully-Fisher slope γ_i). Finally, the dimensionless factor $f(z_s)$ contains all the dependence on cosmology and on the source redshift; for any flat universe ($\Omega_k = 0$), $f(z_s) = D_{os}^3/(30 r_{\rm H}^3)$ (Gott et al. 1989). When considering a population of sources, the cosmology factor f would also include an integral over the source redshift distribution.

We characterize the distribution of lenses using the differential optical depth $d\tau_i/d\theta$, which is equivalent (up to a normalization factor that depends on the cosmology and the source redshift distribution) to a probability distribution for the image separation θ. Hence, we refer to $d\tau_i/d\theta$ as the image separation distribution. It can be evaluated analytically for any flat cosmology,

$$\frac{d\tau_i}{d\theta} = 30 \tau_i^* \, f(z_s) \frac{\hat{\theta}^2}{\theta_i^*} (\Gamma_2 - 2\hat{\theta}\Gamma_4 + \hat{\theta}^2 \Gamma_6) \, , \tag{14}$$

$$\Gamma_n \equiv \Gamma(1 + \alpha_i - n\gamma_i^{-1}; \max(\hat{\theta}^{\gamma_i/2}, L_{\rm cut}/L_i^*)) \, , \tag{15}$$

where $\hat{\theta} = \theta/\theta_i^*$. Moments of this distribution can also be evaluated analytically for any flat cosmology,

$$\langle \theta \rangle_i = \frac{\theta_i^*}{2} \frac{\Gamma(1 + \alpha_i + 6\gamma_i^{-1}; L_{\rm cut}/L_i^*)}{\Gamma(1 + \alpha_i + 4\gamma_i^{-1}; L_{\rm cut}/L_i^*)} \, , \tag{16}$$

$$\langle \theta^2 \rangle_i = \frac{2(\theta_i^*)^2}{7} \frac{\Gamma(1 + \alpha_i + 8\gamma_i^{-1}; L_{\rm cut}/L_i^*)}{\Gamma(1 + \alpha_i + 4\gamma_i^{-1}; L_{\rm cut}/L_i^*)} \, , \tag{17}$$

where $\langle \cdots \rangle_i$ denotes an average over galaxy population i. The mean image separation is simply $\langle \theta \rangle_i$, while the standard deviation is $[\langle \theta^2 \rangle_i - \langle \theta \rangle_i^2]^{1/2}$.

All of these results apply for a single galaxy population in a flat cosmology. For the generalization to arbitrary cosmologies, see Kochanek (1993b). For the generalization to multiple galaxy populations, the linearity of the optical depth means that we can simply sum over populations,

$$\tau_{\rm tot} = \sum_i \tau_i \, , \tag{18}$$

$$\frac{d\tau_{\rm tot}}{d\theta} = \sum_i \frac{d\tau_i}{d\theta} \, . \tag{19}$$

When computing moments of the image-separation distribution, we must be careful to weight the populations correctly,

$$\langle \theta \rangle_{\rm tot} = \frac{\sum_i \tau_i \langle \theta \rangle_i}{\sum_i \tau_i} \, , \tag{20}$$

and similarly for $\langle \theta^2 \rangle_{\rm tot}$.

Finally, all of these results apply to a galaxy population with no redshift evolution other than passive luminosity evolution. However, redshift surveys suggest that there is evolution in the comoving number density of late-type galaxies (Lilly et al. 1995; Lin et al. 1999). Adding number density evolution $n_i^*(z)$ to the statistical results given above is straightforward: evaluate τ_i^* using the local number density $n_i^*(0)$, and replace the cosmology factor $f(z_s)$ with the cosmology/evolution factor

$$f_{\rm evol}(z_s) = \frac{1}{r_{\rm H}^3} \int_0^{D_{os}} \frac{n_i^*(z_l)}{n_i^*(0)} \frac{(D_{ol} D_{ls}/D_{os})^2}{(1 + \Omega_k D_{ol}^2/r_{\rm H}^2)^{1/2}} \, dD_{ol} \, . \tag{21}$$

Note that making an explicit luminosity cut at the LCRS completeness limit $M_R = -17.5 + 5 \log h$ excludes some galaxies and therefore yields an underestimate of the lensing optical depth. The cut is necessary because the luminosity function for any survey is unreliable below the survey's completeness limit. However, the cut does not significantly affect our results, because the faint galaxies below it are very poor lenses. To estimate the amount of optical depth excluded by the cut, consider a GLF that matches an observed GLF about the completeness limit, but is allowed to have an arbitrary slope $\alpha_{\rm faint}$ below the completeness limit. Let $\tau_{\rm bright}$ ($\tau_{\rm faint}$) be the lensing optical depth due to galaxies brighter (fainter) then the completeness limit. Using the C00 sample of NEL galaxies outside groups (see Table 2), we estimate $\tau_{\rm faint}/\tau_{\rm bright} = 0.005$, 0.008, and 0.016 when the slope below the completeness limit is $\alpha_{\rm faint} = -0.5$, -1.0, and -1.5, respectively. In other words, even if the GLF is much steeper below the completeness limit than above the limit, the excluded optical depth is a small fraction of the total.

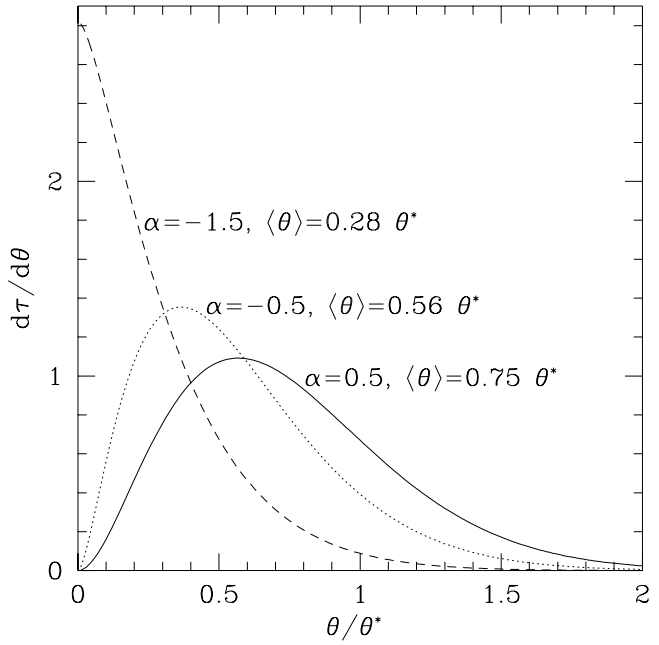

FIG. 1.—Image separation distributions, $d\tau/d\theta$, for environments with different values of the faint-end slope α of the galaxy luminosity function. All the curves use a Faber-Jackson or Tully-Fisher slope $\gamma = 4$ and are normalized to have unit area. The mean image separation $\langle\theta\rangle$ for each curve is indicated.

3. ANALYTIC TRENDS

Before making quantitative predictions about the effects of type and environment in lens statistics, it is instructive to use the analytic results from § 2.3 to identify the general trends. There are two familiar effects related to galaxy type, and two new effects due to the environment.

Because lensing selects galaxies by mass and early-type galaxies tend to be more massive than late-type galaxies, lensing has a strong type selection in favor of early-type galaxies. Equation (11) shows that the lensing optical depth is proportional to $n^*(\sigma^*)^4\Gamma(1 + \alpha + 4\gamma^{-1})$, so the relative number of lenses is expected to be $N(\text{early})/N(\text{late}) \sim 20$, using the data from § 2. Moreover, early-type galaxies tend to produce lenses with larger image separations than late-type galaxies. Equation (16) indicates that the mean image separation $\langle\theta\rangle$ scales as $(\sigma^*)^2$, so $\langle\theta\rangle$ for late-type lenses is only $\sim$20% of that for early-type lenses, although this simple estimate may be complicated by inclination effects due to the thin disk in spiral galaxies (see Maller, Flores, & Primack 1997; Wang & Turner 1997; Keeton & Kochanek 1998). Both of these effects are known from previous calculations of lens statistics (e.g., Turner et al. 1984; Fukugita & Turner 1991). They are also consistent with the data, since most of the more than 50 known lenses are produced by early-type galaxies (e.g., Kochanek et al. 2000a), with only four likely cases of lensing by a spiral galaxy (B0218+357,

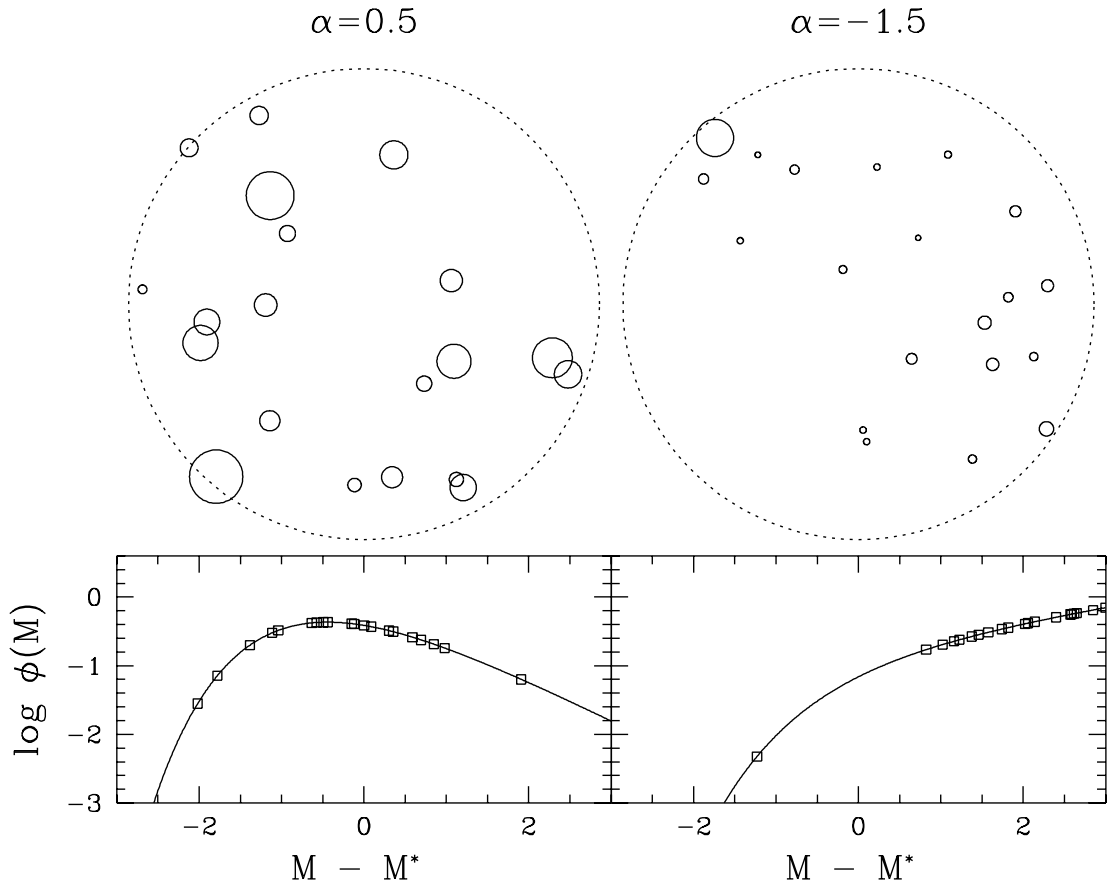

FIG. 2.—Schematic representations of groups with $\alpha = 0.5$ (*left*) and $\alpha = -1.5$ (*right*), normalized to have the same number of galaxies down to $M^* + 3$. The luminosity functions are shown at the bottom. For each group, galaxies are chosen randomly from the luminosity function, placed randomly inside the dotted circle, and drawn with a circle whose area is proportional to the galaxy's luminosity and lensing optical depth and whose diameter is proportional to the image separation. (The random placement of galaxies is not realistic; it is done for illustration only and does not affect our calculations.) The points on the luminosity function indicate the galaxies.

Browne et al. 1993; B1600+434, Jaunsen & Hjorth 1997; PKS 1830−211, Wiklind & Combes 1996; 2237+0305, Huchra et al. 1985). In addition, the smallest known image separation is produced by a face-on spiral galaxy ($\theta = 0\farcs33$ for B0218+357). The type dependence of the number density of lenses and the mean image separation leads to an environmental dependence because of the morphology-density relation, as we show in the next section.

The two new environmental effects arise from the environmental dependence of the faint-end slope α of the GLF. First, because the faint-end slope appears to systematically change with environment (see Tables 1 and 2, and Zabludoff & Mulchaey 2000), the distribution of image separations should vary with environment. Figure 1 shows the image-separation distribution, $d\tau/d\theta$, for different values of α. As α decreases, the distribution becomes more skewed toward small separations, and $\langle\theta\rangle$ decreases. Physically, when α is smaller, the galaxy population has a higher ratio of dwarf galaxies to giant galaxies, which leads to a higher fraction of small-separation lenses.

Second, changes in α with environment affect the numbers of lens and nonlens galaxies differently. Consider Figure 2, which shows schematic representations of groups with $\alpha = 0.5$ and -1.5, normalized to have the same number of galaxies down to $M^* + 3$. If we pick a galaxy at random, it is equally likely to come from either group. However, if we pick a lens galaxy at random, it is far more likely to come from the $\alpha = 0.5$ group than the $\alpha = -1.5$ group, because the latter group is dominated by dwarf galaxies. Considering other toy models, such as groups normalized to have the same lensing optical depth, leads to a general conclusion: other things being equal (i.e., in the absence of a morphology-density relation), lens galaxies are less likely than nonlens galaxies to be found in environments with a large dwarf-to-giant ratio. The effect is probably weaker in observed galaxy populations than in our toy models, with their rather extreme values of α.

4. QUANTITATIVE RESULTS

We now evaluate lens statistics using empirical GLFs to quantify the effects of the morphology-density relation and the dwarf-to-giant ratio on lens statistics. In § 4.1 we present results using the full set of type and environment bins defined by B98 and C00, while in § 4.2 we use coarser binning with only two types (early- and late-type galaxies) and three environments (the field, poor groups, and rich clusters). In § 4.3 we compare our results to the data. In §§ 4.1–4.3 we assume no evolution in the comoving number density of galaxies with redshift, but in § 4.4 we discuss how evolution would affect our results. Finally, in § 4.5 we discuss the effects of possible incompletenesses in the LCRS.

4.1. *Fine Binning*

Figures 3 and 4 show the image-separation distributions $d\tau_i/d\theta$ for the type and environment bins defined by B98 and C00, respectively. The distributions are computed assuming a source redshift $z_s = 2$ and a cosmology with $\Omega_M = 0.3$ and $\Omega_\Lambda = 0.7$. If we were to change the cosmology or the source redshift, or even to allow a distribution of source redshifts, the only effect would be to change $d\tau_i/d\theta$ by

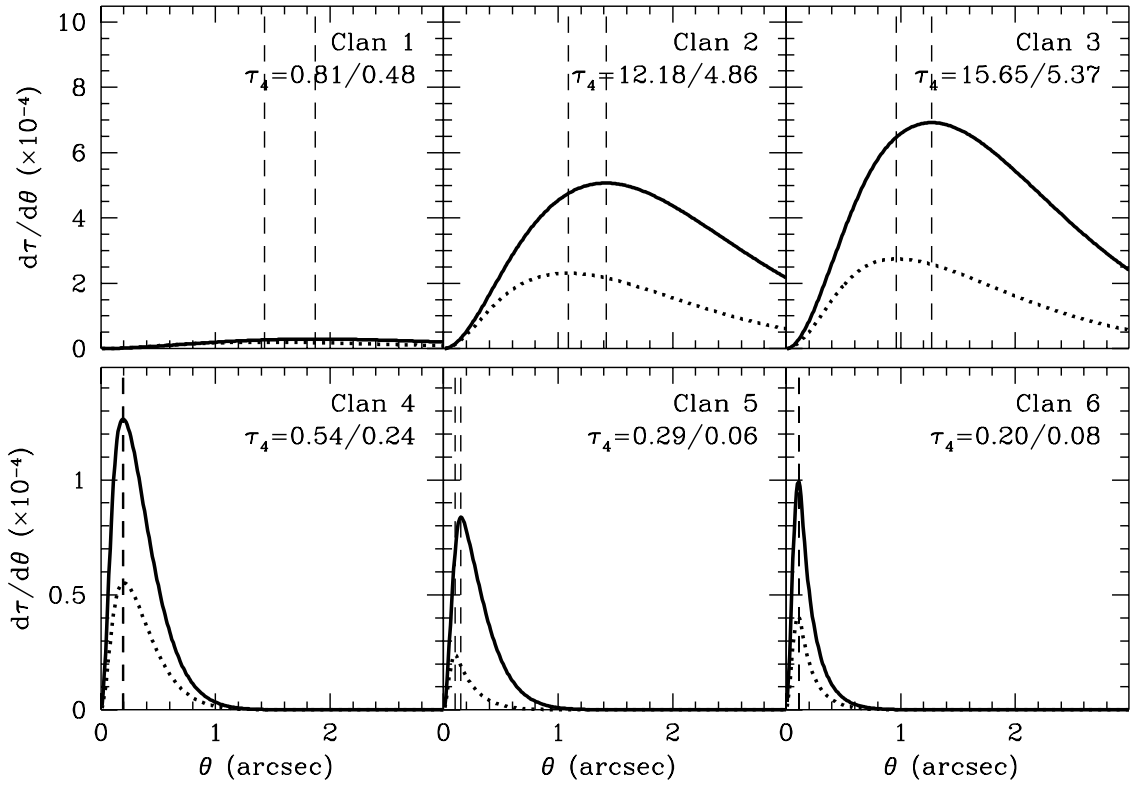

FIG. 3.—Image separation distributions for the six clans and two environments defined by B98. Results are shown for a source at redshift $z_s = 2$ in a cosmology with $\Omega_M = 0.3$ and $\Omega_\Lambda = 0.7$. Each panel contains a single clan; the solid and dotted curves denote low- and high-density environments, respectively. Note that the vertical scales differ between the two rows. The vertical dashed lines indicate the peaks of the distributions. The two values of τ_4 in each panel give the optical depth (in units of 10^{-4}) for low- and high-density environments, respectively. We treat clans 1–3 as early-type galaxies and clans 4–6 as late-type galaxies; if we were to reclassify clan 3 as late-type galaxies, the results would look very similar to the clan 4 panel.

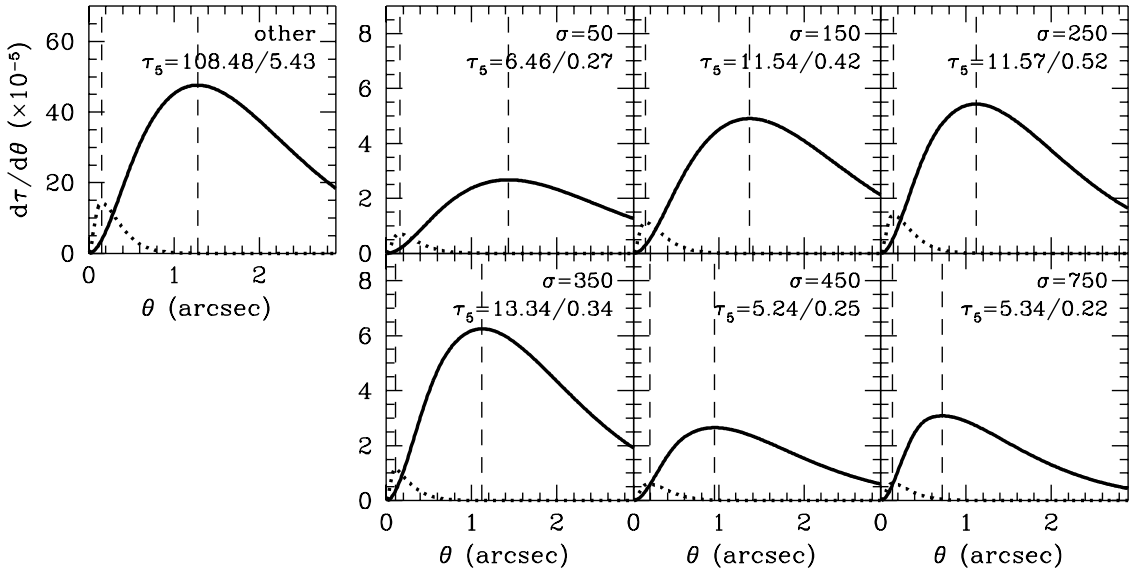

FIG. 4.—Image separation distributions for the two types and seven environments defined by C00, again for $z_s = 2$, $\Omega_M = 0.3$, and $\Omega_\Lambda = 0.7$. Each panel contains a single environment; the solid curves denote NEL galaxies and the dotted curves EL galaxies. The vertical dashed lines indicate the peak of each distribution. In each panel, the two values of τ_5 give the optical depth (in units of 10^{-5}) for NEL and EL galaxies, respectively. Note that the vertical axis scale for the "other" panel differs from that in the group panels. For the luminosity/mass conversions, we treat NEL galaxies as early-type galaxies and EL galaxies as late-type galaxies.

a multiplicative factor that is identical for all type and environment bins (see eq. [11]). The relative contributions of the different bins to the lensing optical depth are independent of the cosmology and source redshift distribution.

The results illustrate the trends identified in § 3. First, for galaxies in a particular environment, both the amplitude and the peak location of the distributions are larger for early-type galaxies than for late-type galaxies; relative to early-type galaxies, late-type galaxies have a much smaller lensing optical depth and produce smaller image separations. Second, for galaxies of a particular type, the lens distributions in denser environments are more dominated by small image separations. This effect occurs because denser environments tend to have a steeper GLF and hence a higher dwarf-to-giant ratio (B98; C00; Zabludoff & Mulchaey 2000), which means a higher fraction of galaxies that produce small-separation lenses. These trends are seen in both the B98 and C00 samples, which suggests that they are not overly sensitive to details of the type and environment classification schemes.

4.2. *Coarse Binning*

The type classification of B98 and the environment classification of C00 both yield finer differentiation than we seek for characterizing the type and environment distributions of lens galaxies. We confine the B98 sample to two type bins by defining an early-type sample using clans 1–3 and a late-type sample with clans 4–6. We reclassify the C00 sample into three environment bins: the field, poor groups, and rich clusters. Studies of groups suggest that many systems with velocity dispersions $\sigma \lesssim 200$ km s^{-1} are either spurious or similar to the Local Group, which is bound but not yet virialized (Diaferio et al. 1993; Zaritsky 1994; Zabludoff & Mulchaey 1998). Hence, to be conservative, we define a "field" bin that contains both galaxies not in groups and galaxies in systems with $\sigma < 200$ km s^{-1}, a "group" bin that contains galaxies in systems with $200 < \sigma < 500$ km s^{-1}, and a "cluster" bin that contains galaxies in systems with $\sigma > 500$ km s^{-1}. As we demonstrate below, our main conclusions are robust to the effects of changing the definitions of the coarse bins. Note that we compute statistical quantities for the full set of type and environment bins, and then combine the results into the coarse bins using equations (18)–(20); we do not try to define a GLF for each coarse bin.

Figure 5 shows the relative contributions of the coarse type and environment bins to the sets of nonlens and lens galaxies. We emphasize that the results for nonlens galaxies are empirical results from observed galaxy samples, while the results for lens galaxies are predictions based on the SIS lens model. The most dramatic result is the familiar type difference between nonlens and lens galaxies. Late-type or EL galaxies account for 66% and 68% of nonlens galaxies in the B98 and C00 samples, respectively, but only 4% of lens galaxies in either sample.[1] Again, these results reiterate the well-known fact that lensing selects galaxies by mass and overwhelmingly favors early-type galaxies.

The environment fractions are given in Table 3. The morphology-density relation is evident in the environment fractions for nonlens galaxies; it can also be seen in the NEL fraction, which for the C00 sample is 0.30, 0.39, and 0.52 in the field, groups, and clusters, respectively. Acting alone, the morphology-density relation would imply that lens galaxies should be more likely than nonlens galaxies to lie in dense environments. However, lensing is also affected by changes in the dwarf-to-giant ratio with environment. It

[1] Changing the type classification of the B98 clan 3 and 4 galaxies would of course change the type fractions. Reclassifying clan 3 galaxies as late-type would increase the fraction of late-type nonlens galaxies to 85% and the fraction of late-type lens galaxies to 11%. Conversely, reclassifying clan 4 galaxies as early-type would reduce the nonlens late-type fraction to 43% and the lens late-type fraction to 1%. The effects are smaller for lens galaxies than for nonlens galaxies because late-type galaxies contribute a small fraction of lenses to begin with.

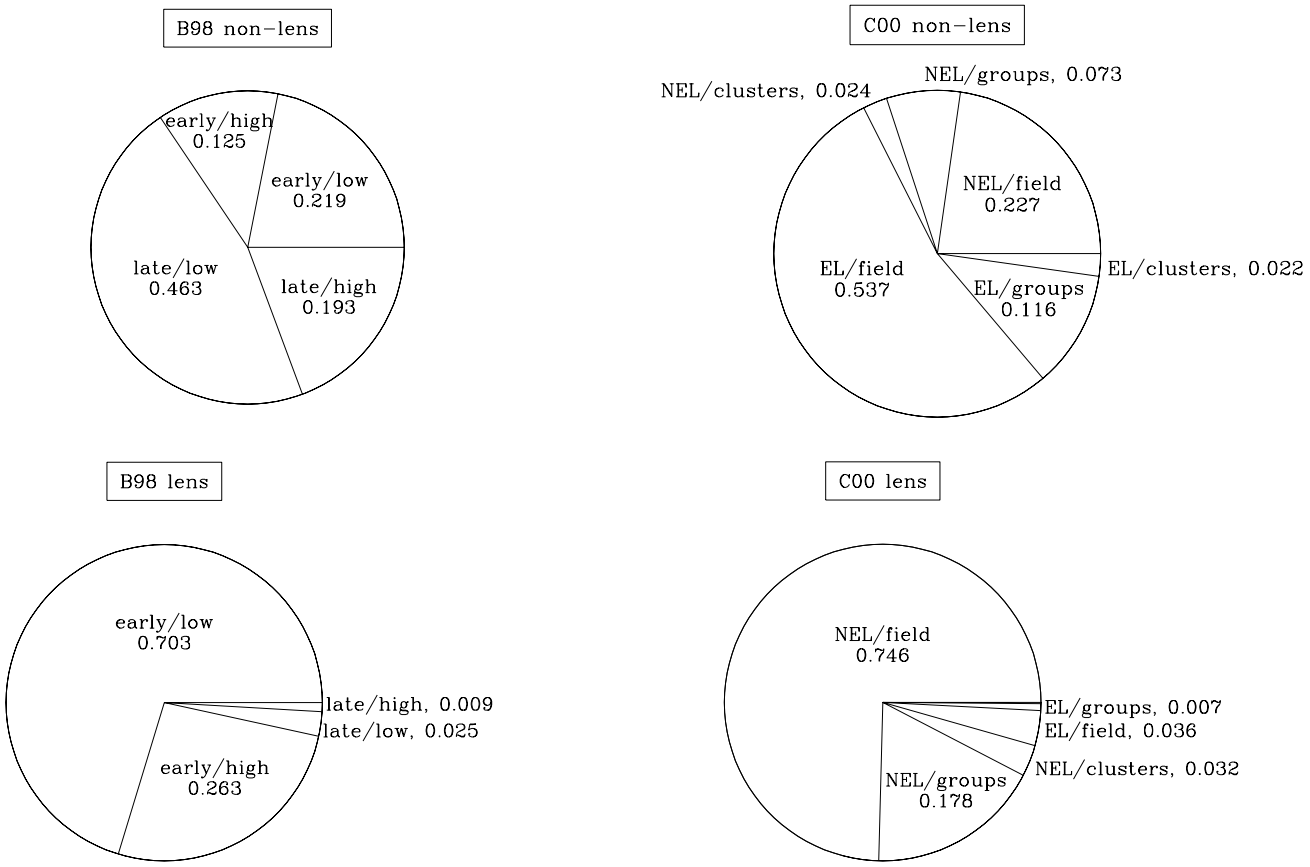

FIG. 5.—Pie charts giving the relative contributions of the different type and environment bins to the set of nonlens galaxies (*top*) and the set of lens galaxies (*bottom*). Results are shown for the B98 (*left*) and C00 (*right*) samples defined in the text. For the C00 lens sample, the EL/clusters bin has a fraction 0.001 and is too small to be seen.

turns out that the two effects nearly cancel, and the environment fractions are very similar for nonlens and lens galaxies. In fact, the changing dwarf-to-giant ratio is the slightly stronger effect. Hence, lens galaxies are slightly less likely than nonlens galaxies to lie in dense environments, although the differences are small and may be hard to detect. The similarity between the results computed with the B98 and C00 samples again suggests that systematic differ-

TABLE 3

ENVIRONMENT FRACTIONS

	B98 SAMPLE		C00 SAMPLE		
GALAXY TYPE	Low-Density	High-Density	Field	Groups	Clusters
Early type:					
Nonlens.....	0.636	0.364	0.700	0.226	0.074
Lens.....	0.728	0.272	0.781	0.186	0.033
Late type:					
Nonlens.....	0.706	0.294	0.796	0.171	0.033
Lens.....	0.733	0.267	0.821	0.149	0.030
All:					
Nonlens.....	0.682	0.318	0.765	0.189	0.046
Lens.....	0.728	0.272	0.783	0.185	0.033

NOTE.—Fraction of nonlens and lens galaxies of different types that are expected in each environment, computed for the samples defined in the text. We use Monte Carlo simulations to estimate the statistical uncertainties in the environment fractions due to measurement uncertainties in α and M^* (given by C00) and σ^* (see § 2.2). We estimate that the uncertainties are ≤ 0.040, 0.037, and 0.023 for nonlens galaxies in the field, groups, and clusters, respectively, while they are ≤ 0.008 for lens galaxies in all environments. These results are robust to changes in the definitions of the type and environment bins. The B98 fractions are essentially unchanged if we change the type classification of clans 3 and/or 4. For the C00 sample, if we increase the lower velocity dispersion threshold for groups to $\sigma = 300$ km s^{-1}, the field, group, and cluster fractions become 0.839, 0.115, and 0.046, respectively, for nonlens galaxies and 0.853, 0.114, and 0.034, respectively, for lens galaxies.

ences in classifying galaxy types and environments have little effect on the relative contributions of different environments to lens statistics.

Quantitatively, we predict that 22%–27% of lens galaxies are in high-density, bound systems such as groups and clusters, and that the majority of these are in poor groups rather than rich clusters. These results are consistent with known lenses; the sample of more than 50 lenses includes four lens galaxies in clusters and three in confirmed groups, but most lens galaxy environments remain undetermined. Our predictions yield a lower limit on the fraction of lens systems in which the lensing potential is probably perturbed by elements other than the lens galaxy. If the lens galaxy lies in a bound group or cluster, it is very likely that other group galaxies and an extended dark matter halo contribute shear and/or convergence to the lensing potential. Even if the lens is not in a bound system, however, there may still be neighboring galaxies or structures along the line of sight that noticeably perturb the lensing potential.

The other trend identified in § 3 is that the mean image separation depends on the faint-end slope α, which varies with environment. Table 4 gives the predicted mean and standard deviation of the image separations for lenses in different environments. We predict that the mean separation for lenses in groups is smaller than the mean for lenses in the field, *under the assumption that the environment does not significantly affect the image separation* (see §2.2). The difference in the means is considerably smaller than the standard deviation, so it would take 20–40 group lenses to detect the difference even at the 1 σ level (assuming that for N items with standard deviation σ the uncertainty in the mean is $\sigma/N^{1/2}$). Given good statistics, however, comparing the mean separations for group lenses and field lenses would provide an excellent test of environmental contributions to lensing. Specifically, an extended dark halo in a group containing a lens can provide extra gravitational focusing that increases the image separation beyond that produced by the lens galaxy alone (e.g., Falco, Gorenstein, & Shapiro 1985). Thus, if observed lenses reveal $\langle\theta\rangle$(groups) $>$ $\langle\theta\rangle$(field), contrary to our prediction, it would provide direct evidence that lenses in groups are significantly affected by group dark halos.

TABLE 4

MEAN IMAGE SEPARATIONS

Sample	Environment	$\langle\theta\rangle$ (arcsec)	σ_θ (arcsec)
B98.....	low-density	1.83	1.04
	high-density	1.57	0.95
C00.....	fiield	1.76	1.02
	groups	1.61	0.96
	clusters	1.30	0.85

NOTE.—Predicted mean $\langle\theta\rangle$ and standard deviation σ_θ of the image separation distributions for lenses in different environments. Monte Carlo simulations indicate that the statistical uncertainties in $\langle\theta\rangle$ are $\sim 0\farcs3$, due almost entirely to uncertainties in σ^* (see § 2.2). However, we are more interested in the difference $\langle\theta\rangle$(field) $-$ $\langle\theta\rangle$(groups), where the uncertainty is only $0\farcs09$, which is due primarily to uncertainties in α. (In the difference quantity, σ^* factors out into a constant scale factor.) Larger surveys such as the Sloan Digital Sky Survey (e.g., Gunn & Weinberg 1995) should reduce this uncertainty to $\lesssim 0\farcs04$ by placing better constraints on α.

4.3. *Comparison with Data*

Figure 6 shows our predictions for the total image separation distribution compared with the data for 49 known lenses from the CASTLES lens database.[2] Such comparisons are sensitive to the source redshift distribution and to cosmological parameters (e.g., Kochanek 1996a, 1996b; Falco et al. 1998; Helbig et al. 1999, and references therein). With the SIS lens model, these dependences appear only in a normalization factor that does not affect the shape of the separation distribution (see eq. [11]), so we avoid complications by normalizing the theoretical curves to 49 total lenses.

Ideally, comparisons between theory and data include a careful account of selection biases, but that is impossible here because Figure 6 includes lenses from many different surveys as well as serendipitous discoveries. Thus, it is somewhat surprising to find that the theoretical curves agree quite well with the data. A Kolmogorov-Smirnov (K-S) test (e.g., Press et al. 1992) cannot distinguish between the data and any of the models. The agreement has little to do with the changes in galaxy populations with environment. Using the environment-independent LCRS GLFs given by Lin et al. (1996) yields a separation distribution very similar to the curves shown in Figure 6. The agreement is also insensitive to environmental perturbations of the lensing potential, which our models neglect. The largest known convergence from a group or cluster enclosing a lens increases the image separation by $\sim 20\%$ (see Bernstein &

[2] The CASTLES lens database (Kochanek et al. 2000b) is available at: http://cfa-www.harvard.edu/glensdata.

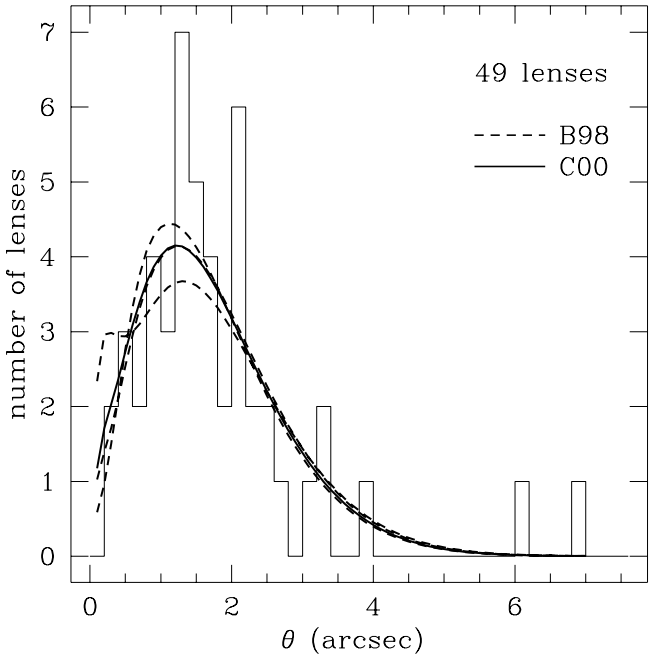

FIG. 6.—Histogram shows the distribution of image separations for 49 known lenses, in bins of width $0\farcs2$. The solid curve shows the net distribution for the C00 sample (a sum of the curves shown in Fig. 4). The three dashed curves show the net distributions for three different models based on the B98 sample. The middle curve represents the model discussed in the text, in which clans 1–3 are treated as early-type galaxies and clans 4–6 as late-type galaxies (a sum of the curves in Fig. 3). In the higher peaked curve, clans 1–4 are treated as early-type galaxies, while in the lower peaked curve, only clans 1–2 are treated as early-type galaxies. All model curves are normalized to 49 lenses, but their shapes are not tuned.

Fischer 1999; Romanowsky & Kochanek 1999). Randomly choosing 25% of the lenses in Figure 6 and increasing their image separations by 20% produces a distribution that is statistically indistinguishable from the original distribution. In other words, examining the image separation distribution without knowing the environments of the lenses is a poor way to test whether environments affect the lensing potential (except in the tail of the distribution, as explained below). A better test is to determine the environments and then compare lenses in groups with lenses in the field, as discussed in § 4.2.

Nevertheless, Figure 6 does offer three conclusions. First, regardless of the selection effects that are at work, it appears that no particular class of lenses is substantially missing. For example, even though finite resolution might bias surveys against finding small-separation lenses, it appears that these lenses are not significantly underrepresented. Second, Figure 6 provides a reassuring consistency check: our addition of population effects to lens statistics has not degraded the agreement between theory and data. It has not substantially improved the agreement, either, because the image separation distribution is not very sensitive to environmental effects, for the reasons just cited.

The third point is that there are two lenses with $\theta > 6''$, RX J0921+4528 and Q0957+561, that lie in the tail of the image separation distribution. The C00 model shown in Figure 6 predicts only 0.04 lenses with $\theta > 6''$ and 1.39 lenses with $\theta > 4''$. Part of the explanation for these two unlikely lenses is that we have neglected environmental contributions to the lensing potential. In Q0957+561 the lens galaxy is the brightest galaxy in a $\sigma \sim 700$ km s^{-1} cluster, and the convergence from the cluster is thought to contribute $\sim$20% of the image separation (e.g., Bernstein & Fischer 1999; Romanowsky & Kochanek 1999). In RX J0921+4528, the lens galaxy appears to be in an X-ray cluster that may likewise contribute to the large separation (Muñoz et al. 2000). These lenses suggest another test of our null hypothesis that potential perturbations do not affect lens statistics. They already indicate that convergence from the environment can be important when the lens lies in a cluster. As the data improve, it will be possible to extend this result to lower mass environments such as groups and determine the importance of including environmental contributions to the lens model in applications of lens statistics.

4.4. *Evolution Effects*

Our results so far have been obtained under the assumption that the comoving number density of galaxies does not change with redshift. However, redshift surveys (e.g., Lilly et al. 1995; Lin et al. 1999) suggest that there is number density evolution, at least in the population of late-type galaxies. (The surveys also imply evolution in the luminosity density, but lensing is insensitive to the component of luminosity density evolution that is due to passive luminosity evolution; see § 2.) To quantify number density evolution, Lin et al. (1999) introduce the parameter P defined by

$$n(z) = n(0)10^{0.4Pz} . \quad (22)$$

In the redshift range $0.12 < z < 0.55$, Lin et al. (1999) find $P \approx 3 \pm 1$ ($1\ \sigma$) for late-type galaxies and essentially no number evolution in early-type galaxies.

We can include the effects of number evolution in the lens statistics by replacing the cosmology factor $f(z_s)$ in equation (11) with the cosmology/evolution factor $f_{\rm evol}(z_s)$ from equation (21), which is equivalent to multiplying the optical depth by an evolution factor $f_{\rm evol}(z_s)/f(z_s)$. Table 5 shows that this factor increases strongly with both the number evolution parameter P and the source redshift z_s. With higher P the evolution is more rapid, and with higher z_s the increase in number density between the observer and the source is larger. Strong number evolution ($P \sim 3$) can increase the optical depth for late-type galaxies to lens a distant source ($z_s \sim 3$) by more than an order of magnitude. The effect is unlikely to be this strong, however, for two reasons. First, fewer than 10% of lenses have sources beyond $z_s = 3$. Second, the strong evolution found by Lin et al. (1999) was measured in the redshift range $0.12 < z < 0.55$; there are no current grounds for extrapolation to $z \sim 1$ or beyond, especially using an exponential function that may overestimate the evolution at high redshifts.

TABLE 5

NUMBER EVOLUTION FACTORS

	z_s			
P	1.5	2.0	2.5	3.0
1.5.....	2.51	3.28	4.23	5.44
2.0.....	3.53	5.17	7.52	11.00
2.5.....	5.05	8.41	14.06	23.90
3.0.....	7.35	14.10	27.56	55.57

NOTE.—Number evolution factor $f_{\rm evol}(z_s)/f(z_s)$ computed for different values of the source redshift, z_s, and the Lin et al. 1999 number evolution parameter P, assuming $\Omega_M = 0.3$ and $\Omega_\Lambda = 0.7$.

Consider a rather dramatic number evolution factor of $f_{\rm evol}(z_s)/f(z_s) = 10$ for late-type galaxies and no number evolution for early-type galaxies. Using the C00 luminosity functions, we then find that late-type galaxies account for 32% of lens galaxies; the rapid number evolution in late-type galaxies simply increases the number of late-type lens galaxies. The mean image separations correspondingly decrease: $\langle\theta\rangle = 1''.33$, $1''.29$, and $1''.03$ for field, group, and cluster lenses, respectively. Nevertheless, the environment fractions are largely unchanged: 79% of lens galaxies in the field, 17% in groups, and 3% in clusters. (Compare with Tables 3 and 4 for the results without number evolution.) The environment distributions for early- and late-type lens galaxies are simply not very different, so changing the relative fraction of lens galaxy types does not significantly change the net distribution of lens galaxy environments.

4.5. *Incompleteness Effects*

All galaxy redshift surveys are incomplete, with either explicit or implicit magnitude and surface brightness limits. Lin et al. (1996) estimate a completeness limit of $M_R = -17.5 + 5 \log h$ for the LCRS, and we have restricted our analysis to galaxies brighter than this limit. We now ask whether any remaining incompletenesses brighter than this limit could affect the lens statistics.

From a direct comparison of the R-band LCRS with the B-band CfA2 redshift survey, Huchra (1999) argues that the LCRS underestimates the number of galaxies with $M_R \lesssim -16 + 5 \log h$ by a factor of $\sim$4, and that most of the "missing" galaxies are low surface brightness, late-type, emission-line galaxies. Although most of the suggested incompleteness occurs at magnitudes fainter than we con-

sider (and fainter than the LCRS completeness limit) and is derived from a perilous comparison of surveys in different bandpasses, we use it to estimate the effects of incompleteness on our analysis.

In § 2.3 we argue that even if the GLF below the completeness limit is much steeper than above the limit, the optical depth from galaxies below the limit is a tiny fraction of the total. Hence, the behavior of the GLF below the completeness limit has essentially no effect on our results. To check our results further, we consider the effects if the LCRS underestimates the number of galaxies even at magnitudes brighter than the completeness limit. We increase the number of galaxies in the $\Delta m = 1$ mag bin above the LCRS completeness limit by the factor of ~ 4 estimated by Huchra (1999). Our approach is conservative, because we apply the changes at magnitudes significantly brighter than where Huchra (1999) proposes most of the incompleteness. If the incompleteness applies to late-type galaxies in all environments, we find that it changes the lens environment fractions by <0.001 compared with Table 3, and it decreases the mean image separations by $\sim 0\farcs02$ compared with Table 4. If the incompleteness applies only to late-type galaxies in the field (because of the morphology-density relation), it changes the lens environment fractions by ~ 0.002 and the mean image separation in the field by $\sim 0\farcs02$. In other words, because it mainly applies to faint galaxies that are poor lenses, incompleteness has a negligible effect on our results.

5. CONCLUSIONS

We have studied how changes in galaxy populations with environment affect gravitational lens statistics, quantifying the results with data from the Las Campanas Redshift Survey (Shectman et al. 1996). Two effects determine how the distribution of lens galaxy environments differs from the distribution of normal galaxy environments. First, the likelihood that lens galaxies lie in groups and clusters is enhanced by the morphology-density relation (e.g., Dressler 1980) and the fact that lensing tends to select massive early-type galaxies. Second, it is diminished by the systematic increase in the fraction of dwarf galaxies relative to giant galaxies in dense environments (e.g., Bromley et al. 1998b; Zabludoff & Mulchaey 2000; Christlein 2000). The two effects nearly cancel, and the fraction of gravitational lens galaxies in a particular environment is very similar to the fraction of nonlens galaxies found in that environment. As a second-order effect, lens galaxies are slightly less likely than nonlens galaxies to be found in poor groups and rich clusters. Quantitatively, we expect $\sim 20\%$ of lens galaxies to be found in poor groups (defined as systems with velocity dispersions in the range $200 < \sigma < 500$ km s^{-1}), and another $\sim 3\%$ of lens galaxies in rich clusters (defined as systems with $\sigma > 500$ km s^{-1}).

Thus, we predict that for $\gtrsim 25\%$ of lenses, the lensing potential may include significant contributions from objects other than the lens galaxy. This result is only a lower limit, for three reasons. First, bound groups may exist below the velocity dispersion threshold of 200 km s^{-1} that we have imposed. Second, a lens that does not lie in a group or cluster can still be perturbed by neighboring galaxies. Finally, lensed images may be perturbed by large-scale structure along the line of sight. External perturbations have been included in models of some individual lenses (e.g., Grogin & Narayan 1996; Schechter et al. 1997; Lehár et al. 2000), but they need to be added to applications of lens statistics, such as limits on Ω_M and Ω_Λ (e.g., Kochanek 1996a; Falco et al. 1998; Helbig et al. 1999). To do so, the statistical analysis of environmental shear by Keeton et al. (1997) must be updated with knowledge of the spatial distribution of galaxies and dark matter in poor groups and rich clusters, not to mention correlations among member galaxies and between galaxies and the diffuse dark halos in groups and clusters. The improved analysis must also include lensing effects that arise from the nonlinear interaction between ellipticity in the lens galaxy and shear from the environment (see Keeton, Mao, & Witt 2000b).

Our calculation provides the starting point for the improved analysis in two ways. First, we have assumed that environmental perturbations of the lensing potential do not affect lens statistics. Subsequent analyses can take our results as the null hypothesis to test whether potential perturbations are important. Second, we have presented empirical tests to determine whether potential perturbations are important statistically. If they are not important, we predict that the mean image separation for lenses in groups is smaller than the mean separation for lenses in the field, although it may take 20–40 group lenses to test this prediction with significance. A contrary empirical result would indicate the presence of extra gravitational focusing, not included in our models, from matter in groups and clusters that is not associated with the lens galaxy. A more immediate version of this test comes from the existence of two large-separation lenses ($\theta > 6''$, RX J0921+4528 and Q0957+561), which is far more than predicted by our models. In fact, both lenses appear to lie in clusters, and in Q0957+561 the cluster is thought to contribute $\sim 20\%$ of the image separation (see Bernstein & Fischer 1999; Romanowsky & Kochanek 1999).

Out of the current sample of about 50 lenses, we expect about 10 lenses in groups and about two lenses in clusters. At present, the environments of most lenses have not been determined. Four lens galaxies appear to lie in clusters (RX J0911+0551, RX J0921+4528, Q0957+561, and HST 1411+5221), and another three in spectroscopically confirmed groups (PG 1115+080, B1422+231, and MG 0751+2716). Once more lensing groups are found, they will provide a sample of groups at redshifts $0.3 \lesssim z \lesssim 1$, which can be compared with existing samples of nearby groups (e.g., Zabludoff & Mulchaey 1998) and of distant clusters (e.g., Stanford, Eisenhardt & Dickinson 1998) to study galaxy evolution in different environments. The existence of lenses in the groups will also permit direct studies of the diffuse dark matter in poor groups of galaxies.

We thank Ben Bromley for providing data in advance of publication, and Huan Lin for helpful discussions. We also thank Chris Kochanek for comments on the manuscript, and the anonymous referee for suggestions that improved the presentation.

REFERENCES

Barkana, R., Lehár, J., Falco, E. E., Grogin, N. A., Keeton, C. R., & Shapiro, I. I. 1999, ApJ, 523, 54
Bernstein, G., & Fischer, P. 1999, AJ, 118, 14
Bromley, B. C., Press, W. H., Lin, H., & Kirshner, R. P. 1998a, ApJ, 505, 25 (B98)
———. 1998b, preprint (astro-ph/9805197) (B98)
Browne, I. W. A., Patnaik, A. R., Walsh, D., & Wilkinson, P. N. 1993, MNRAS, 263, L32
Chae, K.-H. 1999, ApJ, 524, 582
Christlein, D. 2000, ApJ, in press (C00)
Diaferio, A., Ramella, M., Geller, M. J., & Ferrari, A. 1993, AJ, 105, 2035
Dressler, A. 1980, ApJ, 236, 351
Fabbiano, G. 1989, ARA&A, 27, 87
Falco, E. E., Gorenstein, M. V., & Shapiro, I. I. 1985, ApJ, 289, L1
Falco, E. E., Kochanek, C. S., & Muñoz, J. A. 1998, ApJ, 494, 47
Fischer, P., Schade, D., & Barrientos, L. F. 1998, ApJ, 503, L127
Fukugita, M., & Turner, E. L. 1991, MNRAS, 253, 99
Gott, J. R., Park, M.-G., & Lee, H. M. 1989, ApJ, 338, 1
Grogin, N. A., & Narayan, R. 1996, ApJ, 464, 92 (erratum 473, 570)
Gunn, J. E., & Weinberg, D. H. 1995, in Wide Field Spectroscopy and the Distant Universe, ed. S. Maddox & A. Aragón-Salamanca (Singapore: World Scientific), 3
Helbig, P., Marlow, D., Quast, R., Wilkinson, P. N., Browne, I. W. A., & Koopmans, L. V. E. 1999, A&AS, 136, 297
Huchra, J. 1999, in ASP Conf. Ser. 170, Low Surface Brightness Universe, ed. J. I. Davies, C. Impey, & S. Phillipps (San Francisco: ASP), 45
Huchra, J., Gorenstein, M., Kent, S., Shapiro, I., Smith, G., Horine, E., & Perley, R. 1985, AJ, 90, 691
Jaunsen, A. O., & Hjorth, J. 1997, A&A, 317, L39
Kaiser, N., & Tribble, P. 1991, in ASP Conf. Ser. 21, The Space Distribution of Quasars, ed. D. Crampton (San Franciscso: ASP), 304
Keeton, C. R., Falco, E. E., Impey, C. D., Kochanek, C. S., Lehár, J., McLeod, B. A., Rix, H.-W., Muñoz, J. A., & Peng, C. Y. 2000a, ApJ, 542, 74
Keeton, C. R., & Kochanek, C. S. 1997, ApJ, 487, 42
———. 1998, ApJ, 495, 157
Keeton, C. R., Kochanek, C. S., & Falco, E. E. 1998, ApJ, 509, 561
Keeton, C. R., Kochanek, C. S., & Seljak, U. 1997, ApJ, 482, 604
Keeton, C. R., Mao, S., & Witt, H. J. 2000b, ApJ, 537, 697
Kelson, D. D., van Dokkum, P. G., Franx, M., Illingworth, G. D., & Fabricant, D. 1997, ApJ, 478, L13
Kneib, J.-P., Cohen, J. G., & Hjorth, J. 2000, ApJL, submitted (preprint astro-ph/0006106)
Kochanek, C. S. 1993a, ApJ, 419, 12
———. 1993b, MNRAS, 261, 453
———. 1994, ApJ, 436, 56
———. 1995, ApJ, 445, 559
———. 1996a, ApJ, 466, 638
———. 1996b, ApJ, 473, 595
Kochanek, C. S., Falco, E. E., Impey, C. D., Lehár, J., McLeod, B. A., Rix, H.-W., Keeton, C. R, Muñoz, J. A., & Peng, C. Y. 2000a, ApJ, 543, 131
Koopmans, L. V. E., & Fassnacht, C. D. 1999, ApJ, 527, 513
Kundić, T., Cohen, J. G., Blandford, R. D., & Lubin, L. M. 1997a, AJ, 114, 507
Kundić, T., Hogg, D. W., Blandford, R. D., Cohen, J. G., Lubin, L. M., & Larkin, J. E. 1997b, AJ, 114, 2276
Lehár, J., Falco, E. E., Kochanek, C. S., McLeod, B. A., Muñoz, J. A., Impey, C. D., Rix, H.-W., Keeton, C. R., & Peng, C. Y. 2000, ApJ, 536, 584
Lilly, S. J., Tresse, L., Hammer, F., Crampton, D., & Le Fèvre, O. 1995, ApJ, 455, 108
Lin, H., Kirshner, R. P., Shectman, S. A., Landy, S. D., Oemler, A., Tucker, D. L., & Schechter, P. L. 1996, ApJ, 464, 60
Lin, H., Yee, H. K. C., Carlberg, R. G., Morris, S. L., Sawicki, M., Patton, D. R., Wirth, G., & Shepherd, C. W. 1999, ApJ, 518, 533
Maller, A. H., Flores, R. A., & Primack, J. R. 1997, ApJ, 486, 681
Mao, S. 1991, ApJ, 380, 9
Mao, S., & Kochanek, C. S. 1994, MNRAS, 268, 569
Maoz, D., & Rix, H.-W. 1993, ApJ, 416, 425
Muñoz, J. A., et al. 2000, in ASP Conf. Ser., Gravitational Lensing: Recent Progress and Future Goals, ed. T. Brainerd & C. S. Kochanek (San Francisco: ASP), in press
Press, W. H., Teukolsky, S. A., Vetterling, W. T., & Flannery, B. P. 1992, Numerical Recipes in C: The Art of Scientific Computing (2d Ed.; New York: Cambridge Univ. Press)
Quast, R., & Helbig, P. 1999, A&A, 344, 721
Rix, H.-W., Guhathakurta, P., Colless, M., & Ing, K. 1997a, MNRAS, 285, 779
Rix, H.-W., Maoz, D., Turner, E. L., & Fukugita, M. 1994, ApJ, 435, 49
Rix, H.-W., de Zeeuw, P. T., Carollo, C. M., Cretton, N., & van der Marel, R. P. 1997b, ApJ, 488, 702
Romanowsky, A. J., & Kochanek, C. S. 1999, ApJ, 516, 18
Sakai, S., et al. 2000, ApJ, 529, 698
Schechter, P. L. 1976, ApJ, 203, 297
Schechter, P. L., et al. 1997, ApJ, 475, L85
Schneider, P., Ehlers, J., & Falco, E. E. 1992, Gravitational Lenses (Berlin: Springer)
Shectman, S. A., Landy, S. D., Oemler, A., Tucker, D. L., Lin, H., Kirshner, R. P., & Schechter, P. L. 1996, ApJ, 470, 172
Stanford, S. A., Eisenhardt, P. R., & Dickinson, M. 1998, ApJ, 492, 461
Tonry, J. L. 1998, AJ, 115, 1
Tonry, J. L., & Kochanek, C. S. 1999, AJ, 117, 2034
Turner, E. L. 1980, ApJ, 242, L135
Turner, E. L., Ostriker, J. P., & Gott, J. R. 1984, ApJ, 284, 1
van Dokkum, P. G., & Franx, M. 1996, MNRAS, 281, 985
van Dokkum, P. G., Franx, M., Kelson, D. D., & Illingworth, G. D. 1998, ApJ, 504, L17
Vogt, N. P., Forbes, D. A., Phillips, A. C., Gronwall, C., Faber, S. M., Illingworth, G. D., & Koo, D. C. 1996, ApJ, 465, L15
Wallington, S., & Narayan, R. 1993, ApJ, 403, 517
Wang, Y., & Turner, E. L. 1997, MNRAS, 292, 863
Wiklind, T., & Combes, F. 1996, Nature, 379, 139
Witt, H. J., Mao, S., & Keeton, C. R. 2000, ApJ, in press (preprint astro-ph/0004069)
Young, P., Gunn, J. E., Oke, J. B., Westphal, J. A., & Kristian, J. 1981, ApJ, 244, 736
Zabludoff, A. I., & Mulchaey, J. S. 1998, ApJ, 496, 39
———. 2000, ApJ, 539, 136
Zaritsky, D. 1994, in ESO Conf. Proc. 51, The Local Group: Comparative and Global Properties, ed. A. Layden, R. C. Smith, & J. Storm (Garching: ESO), 187